IOP Publishing Journal of Geophysics and Engineering
J. Geophys. Eng. 14 (2017) 368–379 (12pp) https://doi.org/10.1088/1742-2140/aa5af5

McMC-based nonlinear EIVAZ inversion driven by rock physics

Xinpeng Pan[1], Guangzhi Zhang[1,2], Huaizhen Chen[3] and Xingyao Yin[1,2]

[1] School of Geosciences, China University of Petroleum (Huadong), Qingdao, People's Republic of China
[2] Laboratory for Marine Mineral Resources, Qingdao National Laboratory for Marine Science and Technology, Qingdao, People's Republic of China
[3] CREWES, University of Calgary, Alberta, Canada

E-mail: zhanggz@upc.edu.cn

Received 26 March 2016, revised 9 January 2017
Accepted for publication 20 January 2017
Published 24 February 2017

Abstract

A single set of vertically aligned fractures embedded in a purely isotropic background medium may be considered as a long-wavelength effective transversely isotropic medium with a horizontal symmetry axis (HTI). The estimation of fracture weaknesses is essential for characterizing the anisotropy in HTI media. Using the fractured anisotropic rock-physics models and the wide-azimuth seismic data, elastic impedance inversion variation with incident angle and azimuth, or simply 'EIVAZ' for short, can be carried out for the estimation of the normal and tangential fracture weaknesses with the nonlinear Markov chain Monte Carlo (McMC) strategy. Firstly, an inversion method of nonlinear anisotropic elastic impedance (AEI) with the McMC algorithm was proposed, which is used for the inversion of nonlinear AEI information with different angles of incidence and azimuth. Then we extracted the normal and tangential fracture weaknesses directly using the ratio differences of inverted nonlinear AEI data. So we can eliminate the influence of the isotropic background elastic impedance on the anisotropic perturbation elastic impedance and obtain the normal and tangential fracture weaknesses more stably. A test on a 2D over-thrust model shows that the fracture weaknesses are still estimated reasonably with moderate noise. A test on a real data set demonstrates that the estimated results are in good agreement with the results of the well log interpretation, and our McMC-based nonlinear AEI approach appears to be a stable method for predicting fracture weaknesses.

Keywords: fracture weaknesses, rock-physics model, EIVAZ inversion, nonlinear AEI, McMC strategy

(Some figures may appear in colour only in the online journal)

1. Introduction

The dependence of seismic wave velocity on the propagation direction can be defined as the seismic anisotropy, which is a scale-dependent property and confined to the long-wavelength assumption (Thomsen 2002). A single set of vertically aligned fractures embedded in a purely isotropic background medium may be considered as a long-wavelength effective transversely isotropic medium with a horizontal symmetry axis (HTI) (Rüger 1996, Tsvankin and Grechka 2011). Fractures may be treated as the storage space and migration pathway of reservoirs, whose properties can be characterized using the normal and tangential fracture weaknesses (Hsu and Schoenberg 1993, Schoenberg and Sayers 1995, Bakulin *et al* 2000, Shaw and Sen 2006, Liu and Martinez 2012).

Rock-physics models build a bridge between the seismic response and reservoir parameters (Mavko *et al* 2009), so the fractured anisotropic rock-physics models help with the inversion for the anisotropic parameters. Three fracture models have been proposed, including the linear slip model (Schoenberg 1980, 1983, Schoenberg and Sayers 1995), the aligned penny-shaped crack model (Hudson 1980, 1981, Schoenberg and Douma 1988) and the fractured porous medium model (Thomsen 1995, Hudson *et al* 1996). These three models can all describe the relationships between the fracture weaknesses and the fracture parameters, such as

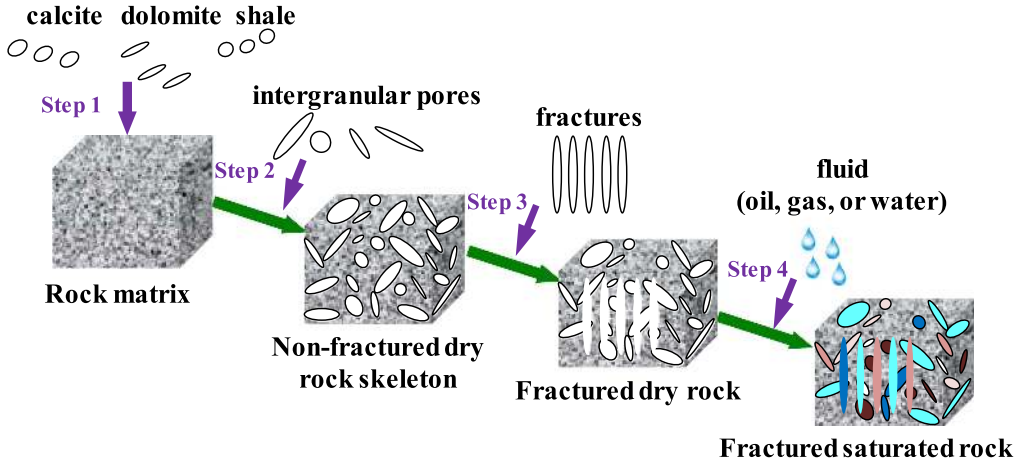

Figure 1. Fractured anisotropic rock-physics model.

fracture density, fracture orientation, pore aspect ratio and pore fluids. For the sake of simplicity, we further assume that the medium is HTI formed by a single set of vertically aligned non-interactive fractures embedded in a purely isotropic background media. With these assumptions, the fracture weaknesses can be derived from the conventional acoustic velocity curves, density curves and other well log information using our improved fractured anisotropic rock-physics effective models (Zhang *et al* 2013, Chen *et al* 2014a).

The stable inversion of the elastic and anisotropic parameters in HTI media may also be a big problem on account of the low signal-to-noise-ratio (SNR) of azimuthal seismic data. Elastic impedance (EI) inversion has been widely used in seismic inversion due to the advantage of angle-stack data, and it can be extended to weakly anisotropic HTI media (Connolly 1999, Whitcombe 2002, Martins 2006, Chen *et al* 2014b). The elastic properties of background isotropic media without fractures, however, do not cause azimuthal changes in the amplitude versus incident and azimuthal angle (AVAZ) data due to the different nature compared to the fracture anisotropic properties, which can cause azimuthal anomalies. Thus simultaneous inversion for the background elastic parameters and fracture anisotropic parameters may be not stable or successful, and the inversion uncertainty of anisotropic parameters is larger than that of background elastic parameters (Far *et al* 2013, Bachrach 2015). Thus the background elastic parameters may be estimated separately, otherwise the fracture anisotropic parameters could be estimated using the azimuthal difference information of EI data. In this paper, a nonlinear anisotropic elastic impedance (AEI) inversion with Markov chain Monte Carlo (McMC) stategy is used for the inversion of nonlinear AEI information with different angles of incidence and azimuth. The normal and tangential fracture weaknesses are then inverted directly using the ratio differences of inverted nonlinear AEI data. So we can eliminate the effects of the isotropic background EI on the anisotropic perturbation EI and obtain the normal and tangential fracture weaknesses more stably. Tests on both the 2D overthrust model and real data demonstrate that the normal and tangential fracture weaknesses may be estimated reasonably, and our method appears to provide an alternative to inverting the normal and tangential fracture weaknesses.

2. Theory

2.1. Linearized PP- wave EIVAZ equation containing fracture weaknesses

Based on the weakly anisotropic theory (Thomsen 1986), Rüger (1996) derived the PP-wave azimuthal reflectivity with the assumption of HTI anisotropy and the same symmetry axes, which can be written as the sum of the isotropic background reflection and the anisotropic perturbation reflection:

$$R_{\mathrm{PP}}(\theta,\phi) = R_{\mathrm{PP}}^{\mathrm{iso}}(\theta) + \Delta R_{\mathrm{PP}}^{\mathrm{ani}}(\theta,\phi), \tag{1}$$

where

$$R_{\mathrm{PP}}^{\mathrm{iso}}(\theta) = \frac{1}{2}\sec^2\theta\frac{\Delta\alpha}{\bar{\alpha}} - 4g\sin^2\theta\frac{\Delta\beta}{\bar{\beta}} + \frac{1}{2}(1-4g\sin^2\theta)\frac{\Delta\rho}{\bar{\rho}}, \tag{2}$$

and

$$\Delta R_{\mathrm{PP}}^{\mathrm{ani}}(\theta,\phi) = \frac{1}{2}\left\{\left[\Delta\delta^{(\mathrm{V})} + 2\left(\frac{2\overline{\beta}}{\overline{\alpha}}\right)^2\Delta\gamma\right]\cos^2\phi\right\}\sin^2\theta + \frac{1}{2}\left\{\begin{matrix}\Delta\varepsilon^{(\mathrm{V})}\cos^4\phi + \\ \Delta\delta^{(\mathrm{V})}\sin^2\phi\cos^2\phi\end{matrix}\right\}\sin^2\theta\tan^2\theta. \tag{3}$$

θ is the incident angle; ϕ is the azimuthal angle; α, β, ρ, $\varepsilon^{(\mathrm{V})}$, $\delta^{(\mathrm{V})}$ and γ are the background isotropic parameters and anisotropic parameters in HTI media, respectively; Δ represents the difference symbol, and $\Delta\delta^{(V)} = \delta_2^{(V)} - \delta_1^{(V)}$, $\Delta\varepsilon^{(V)} = \varepsilon_2^{(V)} - \varepsilon_1^{(V)}$, and $\Delta\gamma = \gamma_2 - \gamma_1$ represent the difference values between the interfaces, the superbars represent the mean values between the interfaces, and $\overline{\alpha}$, $\overline{\beta}$ and $\overline{\rho}$ represent the mean values of background isotropic parameters between the interfaces; $g = (\bar{\beta}/\bar{\alpha})^2$ is the squared ratio of the background S- and P-wave velocity; $R_{\mathrm{PP}}^{\mathrm{iso}}(\theta)$ represents the refection coefficients in the absence of

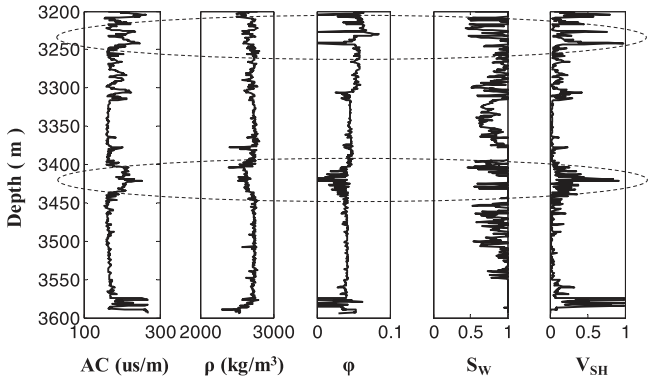

Figure 2. Well log interpretation results. Note that the ellipse indicates the fracture-development zone.

anisotropy, and $\Delta R_{PP}^{ani}(\theta, \phi)$ represents the first-order correction or the anisotropic perturbation for weakly anisotropic media (Martins 2006, Shaw and Sen 2006).

Based on the weakly anisotropic assumption (Thomsen 1986) and Bakulin theory (Bakulin *et al* 2000), the anisotropic parameters can be linearly expressed using the normal and tangential fracture weaknesses Δ_N and Δ_T as

$$\begin{aligned} \varepsilon^{(V)} &\approx -2g(1-g)\Delta_N, \\ \delta^{(V)} &\approx -2g[(1-g)\Delta_N + \Delta_T], \\ \gamma &= \frac{\Delta_T}{2}. \end{aligned} \tag{4}$$

Then substituting equation (4) into equation (1), we get the PP-wave refection coefficient equation in HTI media expressed by the elastic parameters and fracture weaknesses parameters as

$$\begin{aligned} R_{PP}(\theta, \phi) = &\frac{1}{2}a(\theta)\frac{\Delta\alpha}{\bar{\alpha}} + \frac{1}{2}b(\theta)\frac{\Delta\beta}{\bar{\beta}} + \frac{1}{2}c(\theta)\frac{\Delta\rho}{\bar{\rho}} \\ &+ \frac{1}{2}d(\theta, \phi)\Delta_{\Delta_N} + \frac{1}{2}e(\theta, \phi)\Delta_{\Delta_T}, \end{aligned} \tag{5}$$

where

$$\begin{aligned} &a(\theta) = \sec^2\theta; \\ &b(\theta) = -8g\sin^2\theta; \\ &c(\theta) = 1-4g\sin^2\theta; \\ &d(\theta, \phi) = -2g \\ &\quad\times\begin{bmatrix}(\cos^2\phi\sin^2\theta + \sin^2\phi\cos^2\phi\sin^2\theta\tan^2\theta)(1-2g) \\ +(\cos^4\phi\sin^2\theta\tan^2\theta)(1-g)\end{bmatrix}; \\ &e(\theta, \phi) = -g\cos^2\phi\sin^2\theta - 2g\sin^2\phi\cos^2\phi\sin^2\theta\tan^2\theta. \end{aligned} \tag{6}$$

Following the derivation found in Connolly (1999) and Martins (2006), the PP-wave reflection coefficients at horizontal interfaces separating azimuthally anisotropic media can be written as

$$R_{PP}(\theta, \phi) \approx \frac{EI(\theta, \phi)_{n+1} - EI(\theta, \phi)_n}{EI(\theta, \phi)_{n+1} + EI(\theta, \phi)_n} \approx \frac{1}{2}\frac{\Delta EI(\theta, \phi)}{\overline{EI(\theta, \phi)}}, \tag{7}$$

where $n+1$ and n mean the upper and lower interfaces respectively, and EI represents the elastic impedance. Taking the integral of equation (5), we can get a new EIVAZ equation written as

$$\begin{aligned} EI(\theta, \phi) = &EI_0\left(\frac{\alpha}{\bar{\alpha}}\right)^{a(\theta)}\left(\frac{\beta}{\bar{\beta}}\right)^{b(\theta)}\left(\frac{\rho}{\bar{\rho}}\right)^{c(\theta)} \\ &\times \exp(d(\theta, \phi)\Delta_N + e(\theta, \phi)\Delta_T), \end{aligned} \tag{8}$$

where the introduction of EI_0 overcomes the dimensionality dependence on the incidence angle θ (Whitcombe 2002) and $EI_0 = \bar{\rho}\bar{\alpha}$. Based on the perturbation theory (Martins 2006), the EIVAZ equation can also be written as

$$EI(\theta, \phi) = EI^{iso}(\theta)\Delta EI^{ani}(\theta, \phi), \tag{9}$$

where $EI^{iso}(\theta)$ represents the isotropic background EI, and $\Delta EI^{ani}(\theta, \phi) = \exp\left[2\int dR_{PP}^{ani}(\theta, \phi)\right]$ represents the anisotropic perturbation EI. To eliminate the effects of isotropic background EI on the anisotropic perturbation EI, the ratio of anisotropic elastic impedance with different incident angles and azimuthal angles can be expressed as

$$\begin{aligned} \frac{EI(\theta, \phi_j)}{EI(\theta, \phi_i)} &= \frac{\Delta EI^{ani}(\theta, \phi_j)}{\Delta EI^{ani}(\theta, \phi_i)} \\ &= \frac{\exp(d(\theta, \phi_j)\Delta_N + e(\theta, \phi_j)\Delta_T)}{\exp(d(\theta, \phi_i)\Delta_N + e(\theta, \phi_i)\Delta_T)} \quad (j \neq i). \end{aligned} \tag{10}$$

The expression above eliminates the isotropic background EI and only retains the anisotropic perturbation EI.

2.2. McMC-based nonlinear EIVAZ inversion driven by rock-physics models

Due to the limitations of seismic acquisition, the seismic data, and therefore the direct inversion results, do not contain low-frequency components below about 10 Hz, and other information such as well log measurement or stacking velocities should be used to add background low-frequency components. Anisotropy can be caused by rock heterogeneity due to the preferred aligned fractures, thus when the scales of the cracks or the fractures are smaller than the seismic wavelength, the effective-medium theory helps to improve the fractured rock-physics model.

Thus to obtain the nonlinear AEI inversion results with different incident angles and azimuthal angles, we should therefore build a fractured anisotropic rock-physics model to estimate the anisotropic well log information of normal and tangential fracture weaknesses as the complementary low-frequency components. According to the Xu–Payne model (Xu and Payne 2009), we have proposed our fractured anisotropic rock-physics effective model (Zhang *et al* 2013, Chen *et al* 2014a), which is used to estimate the well log information of normal and tangential fracture weaknesses

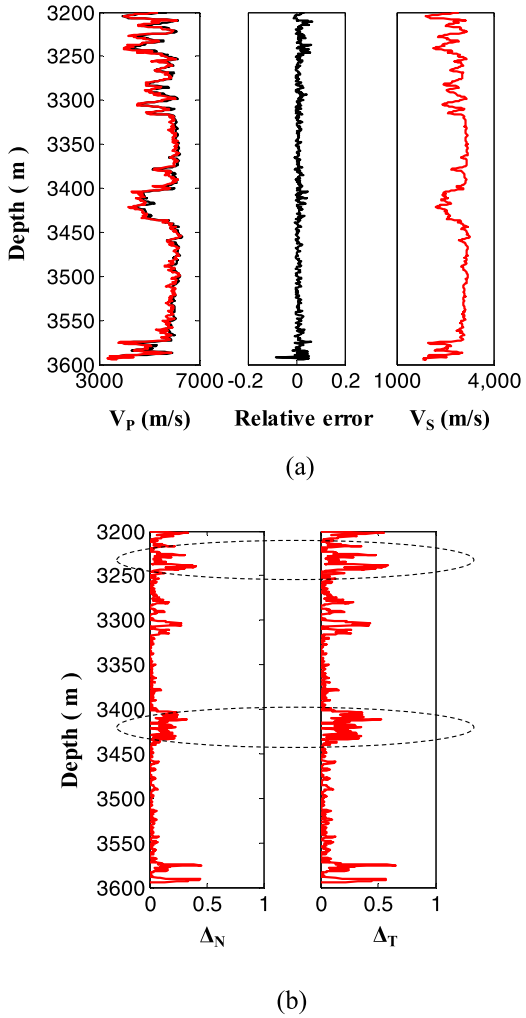

Figure 3. Comparison between the estimated results and true values, where (a) shows the P-wave velocity estimated result and true value and estimated S-wave velocity value, and (b) shows the fracture weakness estimated results. Note that the ellipse indicates the fracture-development zone, the black lines represent the true values and the red lines represent the estimated values.

using the conventional acoustic velocity curves, density curves and other well log information as shown in figure 1.

Step 1. Estimate the elastic modulus of the mineral mixture.

Step 2. Append intergranular pores into the rock matrix and calculate the elastic modulus of the non-fractured dry rock skeleton.

Step 3. Append fractures into the non-fractured dry rock skeleton based on the linear slip model, the aligned penny-shaped cracks model and the fractured porous media model, and then calculate the elastic modulus of the fractured dry rock.

Step 4. Implement the anisotropic fluid substitution in the fractured saturated rock, and finally calculate the fracture normal and tangential weaknesses parameters from the stiffness matrix of the fractured saturated rock.

Brown and Korringa (1975) generalized the isotropic fluid substitution equations to the case where the rock is heterogeneous, which can be written as

$$c_{ijkl}^{\mathrm{sat}} = c_{ijkl}^{\mathrm{dry}} + \frac{(K_0\delta_{ij} - c_{ijaa}^{\mathrm{dry}}/3)(K_0\delta_{kl} - c_{bbkl}^{\mathrm{dry}}/3)}{(K_0/K_{\mathrm{fl}})\phi(K_0 - K_{\mathrm{fl}}) + (K_0 - c_{ccdd}^{\mathrm{dry}}/9)}, \tag{11}$$

where c_{ijkl}^{dry} and c_{ijkl}^{sat} are the effective elastic stiffness element of dry rocks and saturated rocks respectively, K_0 is the mineral bulk modulus, K_{fl} is the fluid bulk modulus, ϕ is porosity, and $\delta_{ij} = \begin{cases} 1 & \text{for } i = j \\ 0 & \text{for } i \neq j \end{cases}$.

In our steps of building a fractured anisotropic rock-physics model, we use equation (11) to calculate the effective elastic stiffness element of fractured saturated rock. Thus the normal and tangential fracture weakness parameters can be calculated using the stiffness matrix of the saturated fractured rock as

$$\Delta_N = \frac{C_{33}^{\mathrm{sat}}(C_{11}^{\mathrm{sat}} - C_{33}^{\mathrm{sat}})}{4C_{55}^{\mathrm{sat}}(C_{55}^{\mathrm{sat}} - C_{33}^{\mathrm{sat}})},$$
$$\Delta_T = 2\frac{C_{55}^{\mathrm{sat}} - C_{44}^{\mathrm{sat}}}{2C_{44}^{\mathrm{sat}}}. \tag{12}$$

The well log information of the normal and tangential fracture weakness parameters proposed in this paper can be estimated from equation (12), and this estimate can be used to establish the low-frequency background model in the AEI inversion. Then we can obtain the nonlinear AEI with different incident angles and azimuthal angles based on the McMC method proposed by Pan *et al* (2015) using the estimated well log information of fracture normal and tangential weaknesses to build the initial model and supplement the low-frequency components.

2.3. Direct extraction for fracture weaknesses

To obtain the linear expression between the fracture weaknesses and the ratio of nonlinear AEI with different incident angles and azimuthal angles, we can use the logarithmic expression written as

$$\ln\left[\frac{\Delta\mathrm{EI}^{\mathrm{ani}}(\theta, \phi_j)}{\Delta\mathrm{EI}^{\mathrm{ani}}(\theta, \phi_i)}\right] = [d(\theta, \phi_j) - d(\theta, \phi_i)]\Delta_N + [e(\theta, \phi_j) - e(\theta, \phi_i)]\Delta_T (j \neq i). \tag{13}$$

In order to highlight the ratio differences of the anisotropic perturbation EI, $\Delta\mathrm{EI}^{\mathrm{ani}}(\theta, \phi_j)$ is chosen to highlight the differences between the azimuthally elastic impedance as far as possible. Assuming that five azimuthally anisotropic elastic impedances are inverted based on the McMC method, we can extract the fracture normal and tangential weaknesses directly

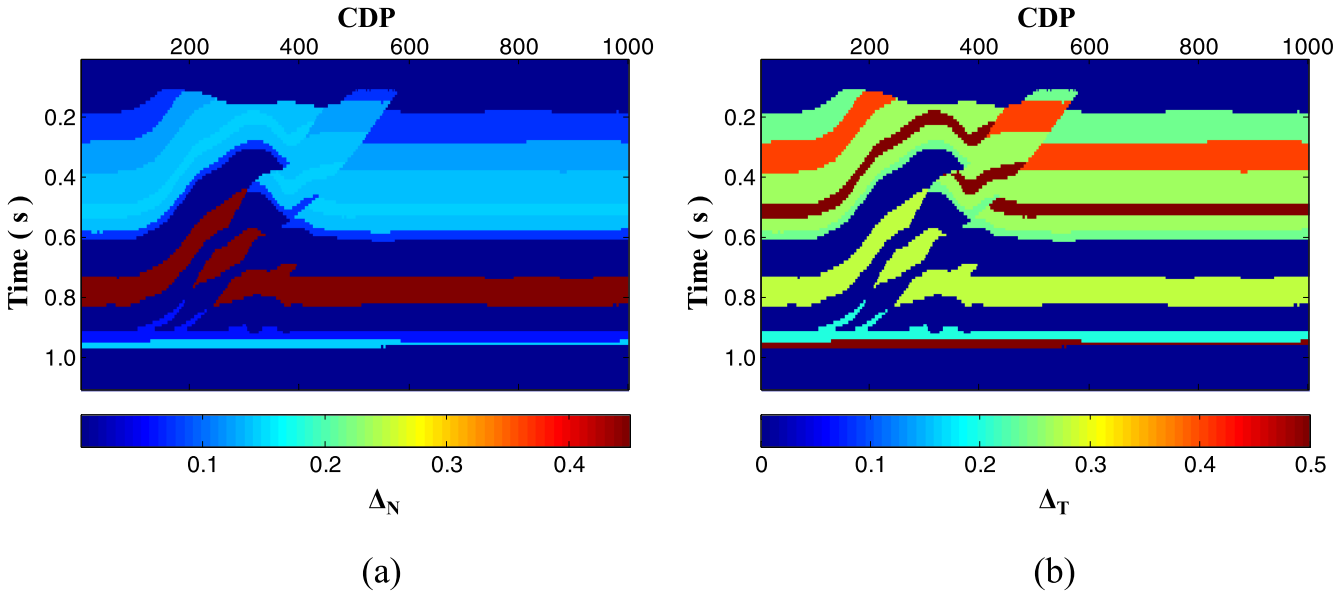

Figure 4. True fracture weaknesses of the over-thrust model, where (a) normal fracture weakness Δ_N and (b) tangential fracture weakness Δ_T.

using the equation written as

$$\begin{cases} \ln\left[\dfrac{\Delta \mathrm{EI}^{\mathrm{ani}}(\theta,\phi_2)}{\Delta \mathrm{EI}^{\mathrm{ani}}(\theta,\phi_1)}\right] = [d(\theta,\phi_2) - d(\theta,\phi_1)]\Delta_N \\ \qquad\qquad + [e(\theta,\phi_2) - e(\theta,\phi_1)]\Delta_T \\ \ln\left[\dfrac{\Delta \mathrm{EI}^{\mathrm{ani}}(\theta,\phi_3)}{\Delta \mathrm{EI}^{\mathrm{ani}}(\theta,\phi_1)}\right] = [d(\theta,\phi_3) - d(\theta,\phi_1)]\Delta_N \\ \qquad\qquad + [e(\theta,\phi_3) - e(\theta,\phi_1)]\Delta_T \\ \ln\left[\dfrac{\Delta \mathrm{EI}^{\mathrm{ani}}(\theta,\phi_4)}{\Delta \mathrm{EI}^{\mathrm{ani}}(\theta,\phi_1)}\right] = [d(\theta,\phi_4) - d(\theta,\phi_1)]\Delta_N \\ \qquad\qquad + [e(\theta,\phi_4) - e(\theta,\phi_1)]\Delta_T \\ \ln\left[\dfrac{\Delta \mathrm{EI}^{\mathrm{ani}}(\theta,\phi_5)}{\Delta \mathrm{EI}^{\mathrm{ani}}(\theta,\phi_1)}\right] = [d(\theta,\phi_5) - d(\theta,\phi_1)]\Delta_N \\ \qquad\qquad + [e(\theta,\phi_5) - e(\theta,\phi_1)]\Delta_T \end{cases}. \quad (14)$$

Equation (14) can be written in matrix form as

$$\boldsymbol{\Omega} = \mathbf{G}\mathbf{m}, \quad (15)$$

where

$$\boldsymbol{\Omega} = \left[\ln\left[\frac{\Delta \mathrm{EI}^{\mathrm{ani}}(\theta,\phi_2)}{\Delta \mathrm{EI}^{\mathrm{ani}}(\theta,\phi_1)}\right], \ln\left[\frac{\Delta \mathrm{EI}^{\mathrm{ani}}(\theta,\phi_3)}{\Delta \mathrm{EI}^{\mathrm{ani}}(\theta,\phi_1)}\right], \ln\left[\frac{\Delta \mathrm{EI}^{\mathrm{ani}}(\theta,\phi_4)}{\Delta \mathrm{EI}^{\mathrm{ani}}(\theta,\phi_1)}\right], \ln\left[\frac{\Delta \mathrm{EI}^{\mathrm{ani}}(\theta,\phi_5)}{\Delta \mathrm{EI}^{\mathrm{ani}}(\theta,\phi_1)}\right]\right]^T,$$

$$\mathbf{m} = [\Delta_N, \Delta_T]^T,$$

$$\mathbf{G} = \begin{bmatrix} d(\theta,\phi_2) - d(\theta,\phi_1) & e(\theta,\phi_2) - e(\theta,\phi_1) \\ d(\theta,\phi_3) - d(\theta,\phi_1) & e(\theta,\phi_3) - e(\theta,\phi_1) \\ d(\theta,\phi_4) - d(\theta,\phi_1) & e(\theta,\phi_4) - e(\theta,\phi_1) \\ d(\theta,\phi_5) - d(\theta,\phi_1) & e(\theta,\phi_5) - e(\theta,\phi_1) \end{bmatrix}. \quad (16)$$

If we solve equation (15), some sampling points of the fracture weaknesses inverted may be extremely unstable, resulting in a discrepancy of the actual geological characteristics. Since the anisotropic perturbation elastic impedances are from the inverted nonlinear elastic impedance, so we can fit regress equation (15) to get the constant coefficient matrix **G** based on the least square (LS) method or the singular value decomposition (SVD) method using the inverted nonlinear anisotropic elastic impedance and the known logging information of the fracture normal and tangential weaknesses. Finally, we can obtain the fracture weaknesses **m**.

2.4. Workflow of McMC-based nonlinear EIVAZ inversion driven by rock physics

Here, we conclude the whole process of McMC-based nonlinear EIVAZ inversion driven by rock physics proposed in this paper as follows.

(1) Pretreatment of the azimuthally pre-stack seismic data and well log data.
(2) Estimation of the well log information about the normal and tangential fracture weaknesses based on the fractured anisotropic rock-physics model.
(3) Accurate extraction of multiple wavelets with different incident angles and azimuthal angles from azimuthal pre-stack seismic data.
(4) Inversion of the nonlinear AEI with different incident angles and azimuthal angles based on the McMC method using the azimuthal angle-stack seismic data and multiple wavelets.
(5) Extraction of the normal and tangential fracture weaknesses directly from the inverted nonlinear AEI with different incident angles and azimuthal angles as the mirror of the reservoir fracture development location.

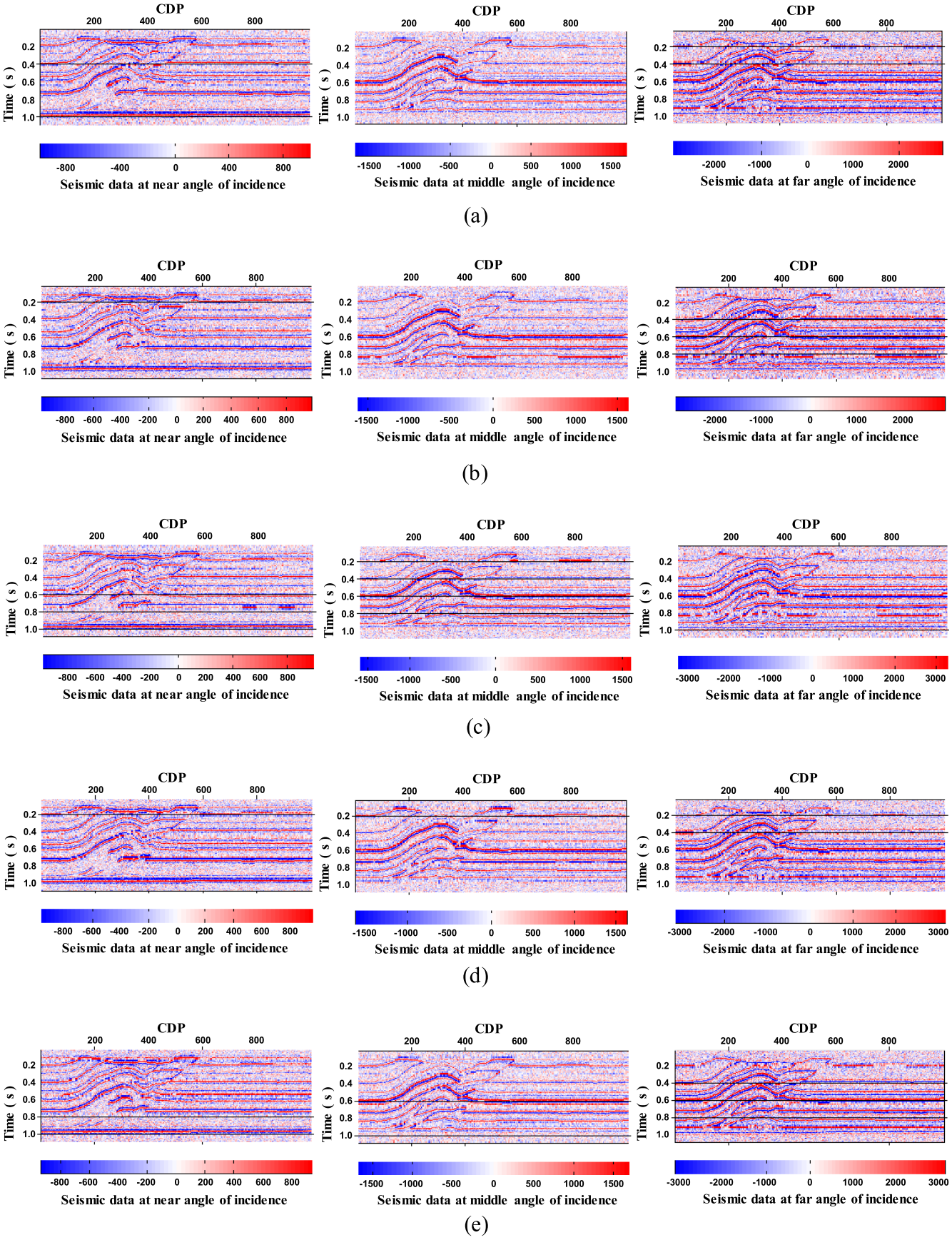

Figure 5. Azimuthal seismic data profiles at different azimuth angles: (a) 0°, (b) 45°, (c) 90°, (e) 135° and (f) 180°.

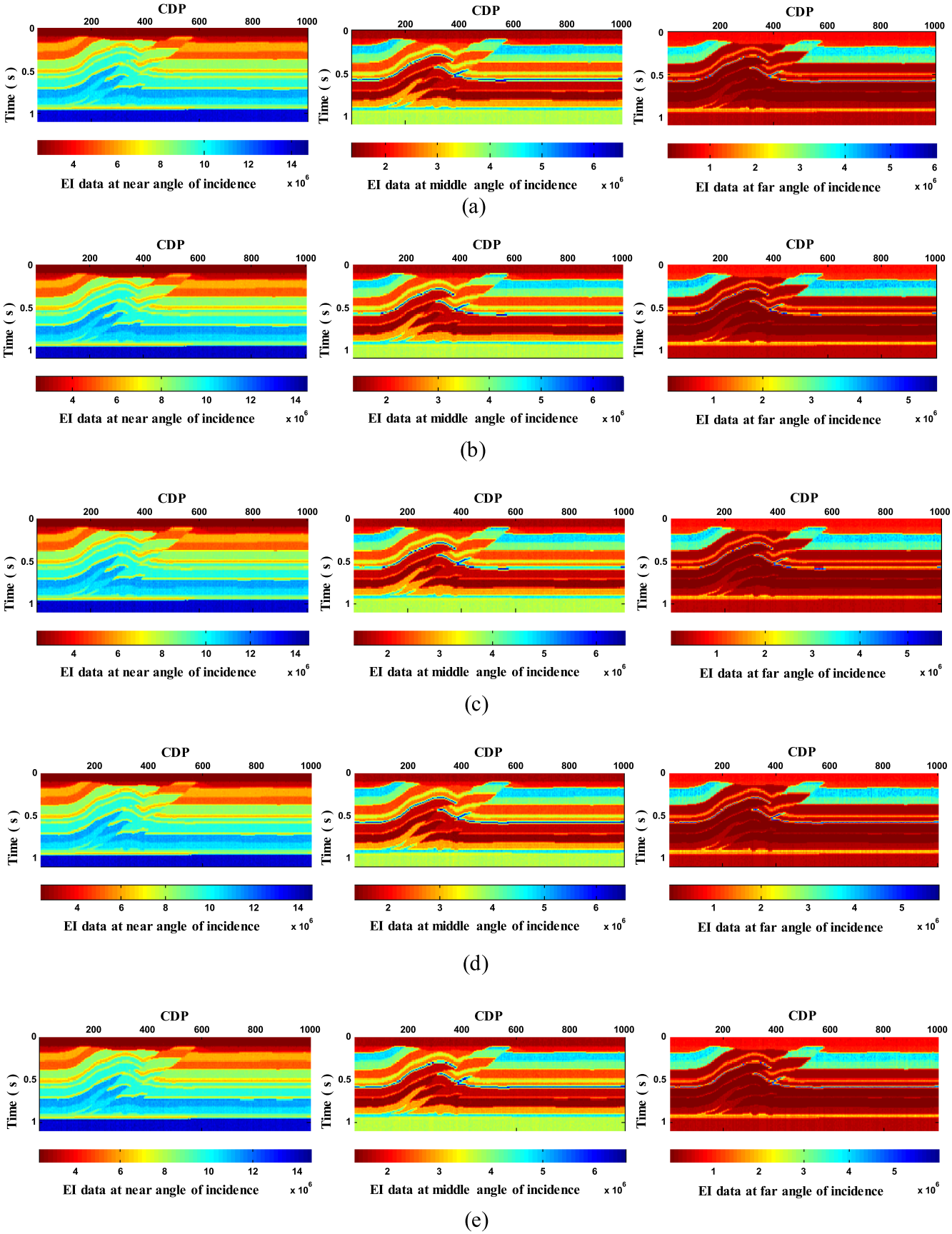

Figure 6. Inverted nonlinear AEI at different azimuth angles: (a) 0°, (b) 45°, (c) 90°, (e) 135° and (f) 180°. Note that the units of nonlinear AEI at different azimuth angles are all kg $m^{-3} \times m\ s^{-1}$.

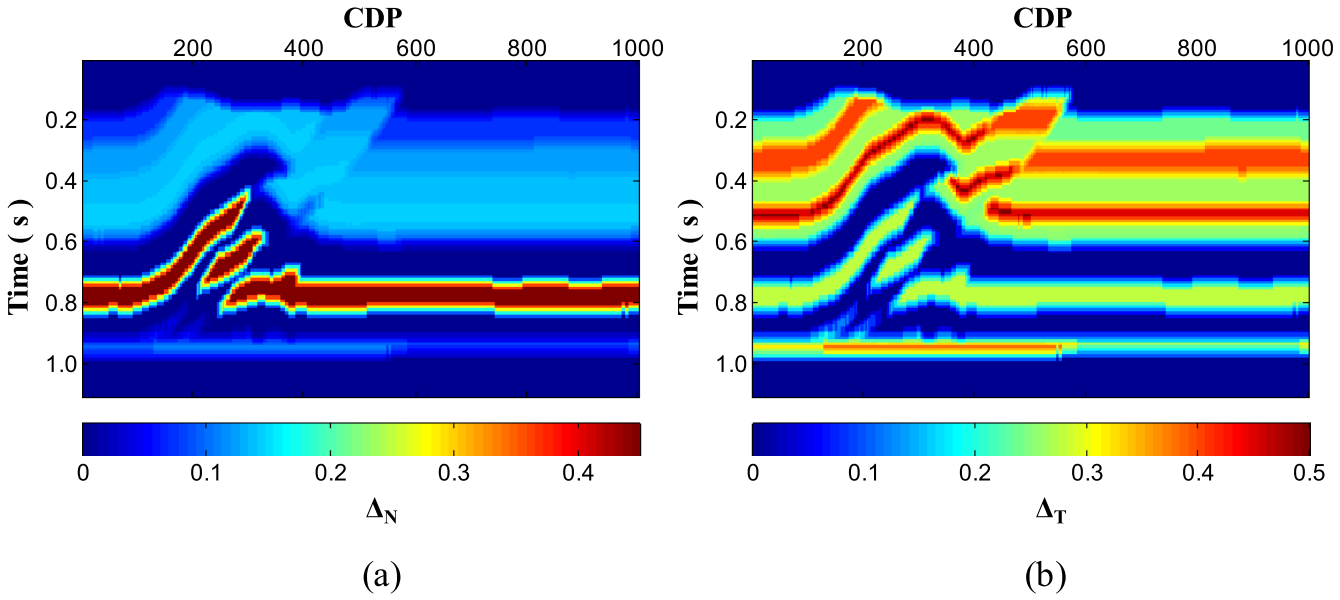

Figure 7. Inverted fracture weaknesses based on the nonlinear EIVAZ inversion, where (a) normal fracture weakness Δ_N and (b) tangential fracture weakness Δ_T.

3. Example

3.1. Estimation of fracture weaknesses based on fractured anisotropic rock-physics model

Well A from a work area of a fractured carbonate reservoir is used to validate the built fractured anisotropic rock-physics models. The fracture weakness parameters including the normal and tangential fracture weaknesses are calculated from conventional well log data using the fractured anisotropic rock-physics models. The estimated results can provide an initial constraint for supplementing the low-frequency components.

Figure 2 shows the data of well log interpretation: acoustic slowness curve (AC), density curve (ρ), porosity curve (φ), water saturation curve (Sw) and clay content curves (Vsh). They are treated as the input of the fractured anisotropic rock-physics models. Figure 3(a) is the P-wave velocity comparison between the estimated result and true value and the estimated S-wave velocity value. Figure 3(b) shows the estimated results of the normal and tangential fracture weakness parameters.

3.2. 2D over-thrust model

To demonstrate that the method proposed in this paper can be used in the case of a complicated anisotropic geological structure, we use the 2D over-thrust models constructed by Aminzadeh *et al* (1997) and Mulder *et al* (2006) to perform the McMC-based nonlinear EIVAZ inversion for the normal and tangential fracture weaknesses. Constant properties were assigned to each of the 16 layers, six of those were transverse isotropic media, defined by the Thomson parameters. The synthetic azimuthal seismic data used the 35 Hz Ricker wavelets and added SNR = 2 random noise. The true model and synthetic azimuthal seismic angle are shown in figures 4 and 5. Figures 6 and 7 are the inverted nonlinear AEIs with different incidence angles and azimuth angles and the normal and tangential fracture weaknesses, respectively.

From the final results of nonlinear AEIs with different incidence angles and azimuth angles and fracture weaknesses, we can see that the inverted results agree with the true model. Moreover, they not only reflect the boundary characteristics of the complicated over-thrust models, but also have a better lateral continuity. Thus the method proposed in this paper appears to provide an alternative to estimate the normal and tangential fracture weaknesses in the over-thrust models.

3.3. Real seismic data

Real pre-stack seismic data located in eastern China are used to validate the reliability of the proposed McMC-based nonlinear EIVAZ inversion method. The five azimuthal seismic data are 172°, 135°, 98°, 61°, and 27°, respectively. Of course, the target reservoir belongs to the carbonate fractured reservoir. To enhance the signal-to-noise ratio of the seismic data, we implement the EIVAZ inversion using the partial angle-stack seismic data. Before implementing the McMC-based nonlinear EIVAZ inversion, the seismic data used should be processed to preserve the amplitude response and remove noise, trying to preserve the amplitudes of the true subsurface reflecting interfaces. The azimuthal seismic data are shown in figure 8, and the inverted nonlinear AEI with different incident angles and azimuthal angles are shown in figure 9. The final results of the fracture weaknesses are shown in figure 10.

The fracture weaknesses can characterize the anisotropy in fractured reservoirs, which are affected by the formation lithology, the fracture development and the pore fluids. In terms of the target reservoir, the formation lithology is composed primarily of marlstone and remains stable. In addition,

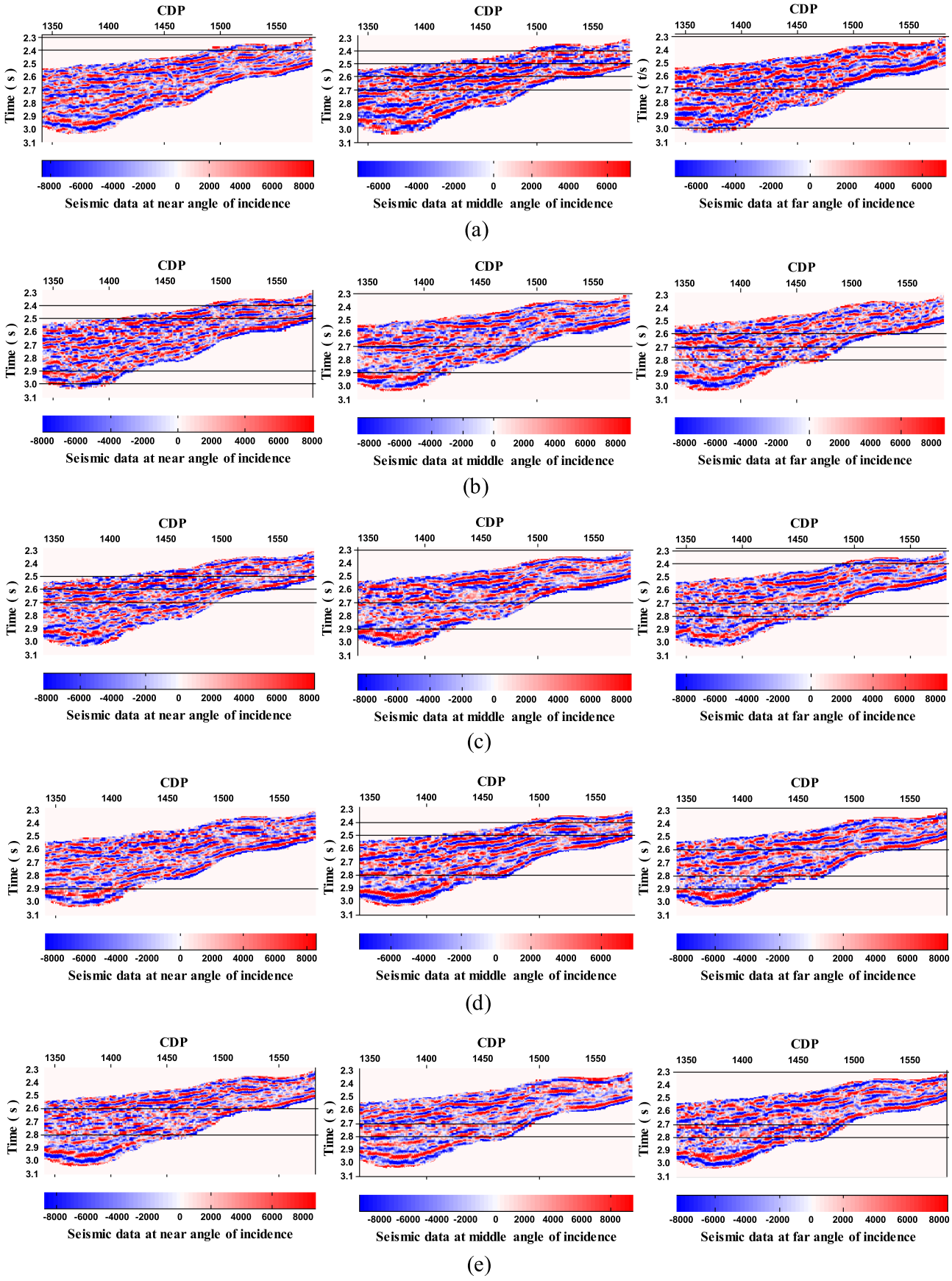

Figure 8. Azimuthal seismic data profiles at different azimuth angles: (a) 172°, (b) 135°, (c) 98°, (e) 61° and (f) 27°.

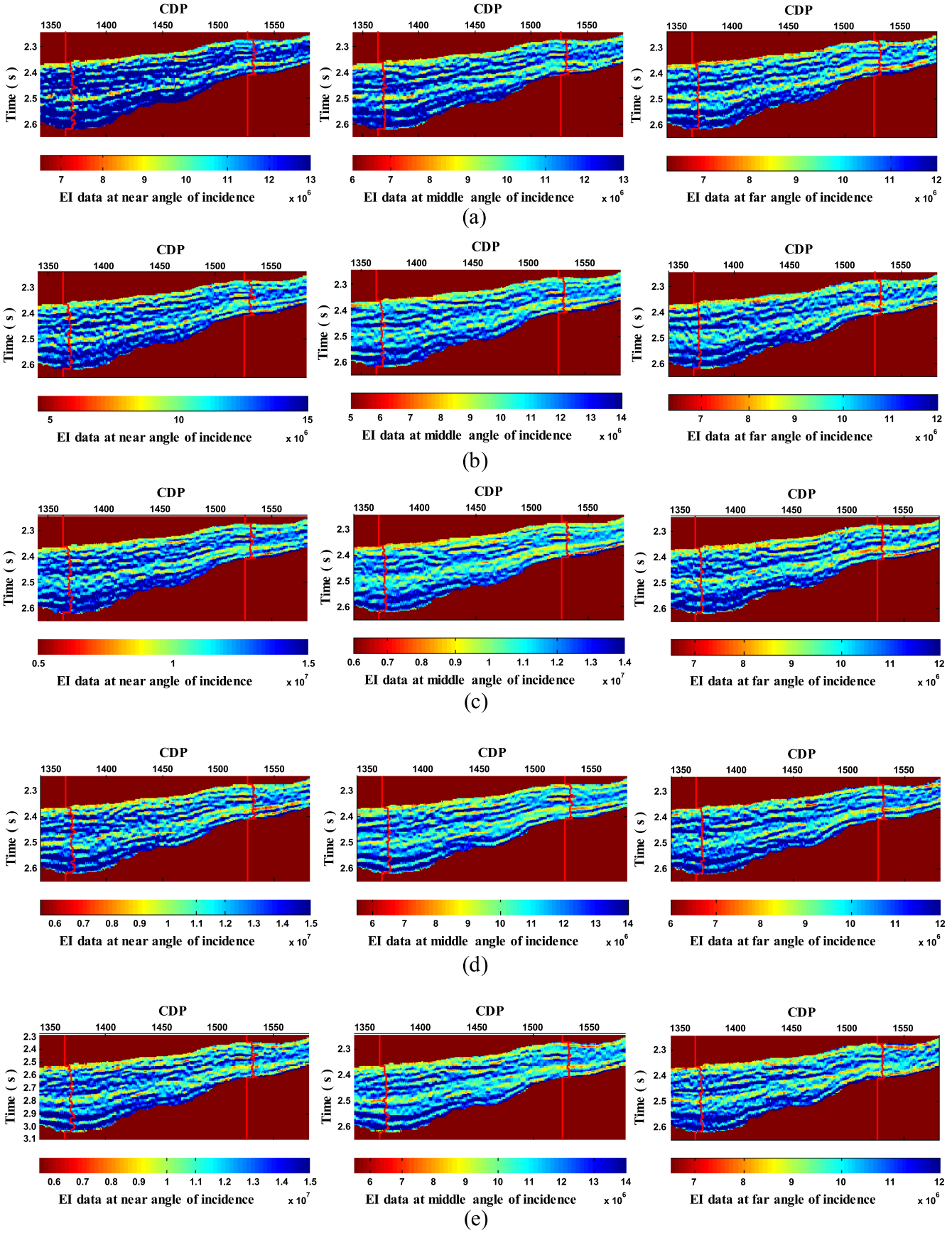

Figure 9. Inverted nonlinear AEI at different azimuth angles: (a) 172°, (b) 135°, (c) 98°, (e) 61° and (f) 27°. Note that the units of nonlinear AEI at different azimuth angles are all kg $m^{-3} \times m\ s^{-1}$, and the log curves in figures are estimated AEI well log information using the built fractured anisotropic rock-physics models.

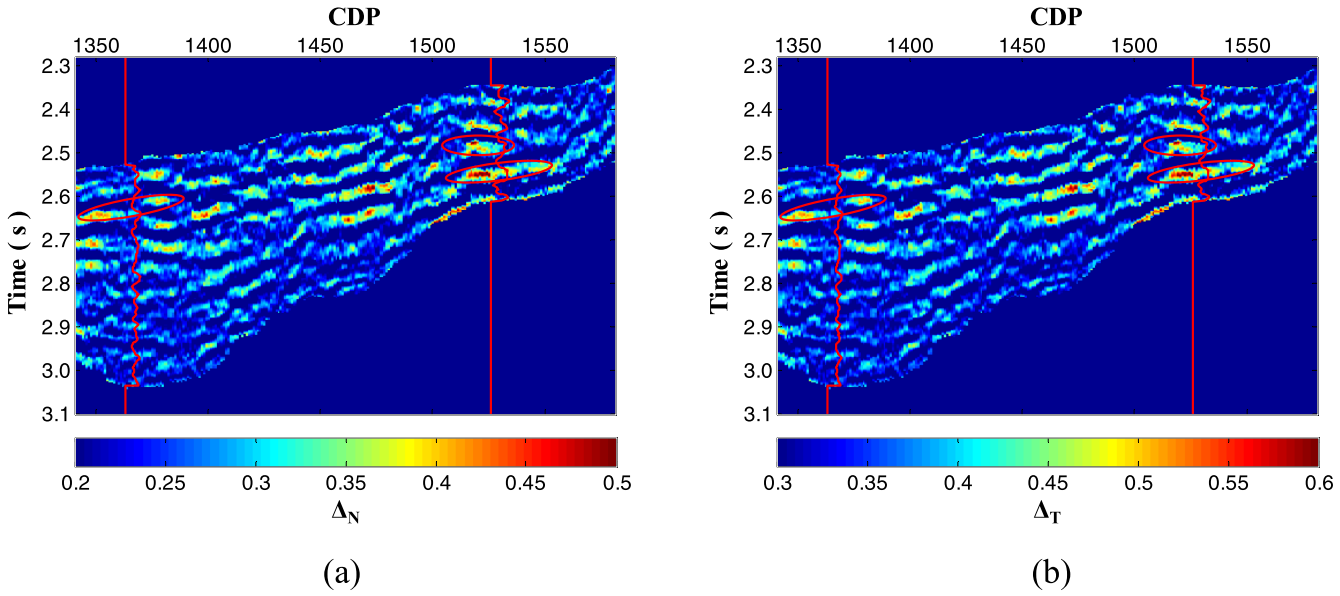

Figure 10. Inverted fracture weaknesses using the nonlinear EIVAZ inversion, where (a) normal fracture weakness Δ_N and (b) tangential fracture weakness Δ_T. Note that the log curves in figures are estimated well log information of the normal and tangential fracture weaknesses driven by the built fractured anisotropic rock-physics models.

the buried depth of the target reservoir is relatively deep. The target belongs to a low-porosity and low-permeability tight carbonate reservoir, whose heterogeneity is strong and has the complex reservoir space types. Thus there is weaker influence of pore fluids on the fracture development. Therefore, we think that the weakness parameters in this area are mainly affected by the fractures, and the numerical size reflects the development degree of the fractures.

From figure 9, we find that the inverted nonlinear AEIs with different incidence angles and azimuth angles based on the McMC strategy have high precision, and agree with the results of an oil-bearing reservoir in the well log interpretation. The red circles in figure 10 represent the fracture development zones, and are also the oil-bearing reservoir area. From the inverted results of fracture weaknesses, we can see that the inverted values agree with the well log data and match the geological characteristics of fracture reservoir development well. So the inverted normal and tangential fracture weaknesses can reflect the reservoir fracture development location. In the fractured oil-bearing reservoir, the fracture weaknesses can also characterize the oil reservoir because we consider that the zones with fractures can be taken as the oil reservoir, where the fracture weaknesses represent the high values. But the average values of fracture weaknesses in the oil-bearing reservoir are different due to the diverse natures of fractured reservoirs. In this fracture-developed work area, the average values of normal and tangential fracture weaknesses are about 0.4 and 0.5, respectively.

4. Conclusions

A single set of vertically aligned fractures embedded in a purely isotropic background medium may be considered as a long-wavelength effective HTI medium. Using the fractured anisotropic rock-physics models and the wide-azimuth seismic data, EIVAZ inversion was proposed for the estimation of the normal and tangential fracture weaknesses with the nonlinear McMC strategy, which were inverted directly using the ratio differences of inverted nonlinear AEI data to eliminate the influence of the isotropic background EI on the anisotropic perturbation EI. Synthetic and real data examples confirm the validity of the proposed method. Thus our method appears to provide an alternative to estimate the normal and tangential fracture weaknesses in fractured reservoirs. However, there are some limitations to the final results: only one inverted result of the fracture weaknesses can be obtained and may lack the uncertainty analysis of the fracture weaknesses. So we will continue our research in this field.

Acknowledgments

We would like to express our gratitude for the sponsorship of the National Natural Science Foundation of China (41674130, U1562215), the National Basic Research Program of China (973 Program, 2013CB228604, 2014CB239201), the National oil and gas major projects of China (2016ZX05027004-001, 2016ZX05002005-009) and the Fundamental Research Funds for the Central Universities (15CX08002A) for their funding this research. We also thank the anonymous reviewers for their constructive suggestions.

References

Aminzadeh F, Brac J and Kunz T 1997 3D salt and overthrust models *Applications of 3-D Seismic Data to Exploration and Production* (*AAPG Studies in Geology No. 42 and SEG Geophysical Developments Series No. 5*) (Tulsa, OK: AAPG/SEG)

Bachrach R 2015 Uncertainty and nonuniqueness in linearized AVAZ for orthorhombic media *The Leading Edge* **34** 1048–50 1052, 1054, 1056

Bakulin A, Grechka V and Tsvankin I 2000 Estimation of fracture parameters from reflection seismic data—part I: HTI model due to a single fracture set *Geophysics* **65** 1788–802

Brown R and Korringa J 1975 On the dependence of the elastic properties of a porous rock on the compressibility of the pore fluid *Geophysics* **40** 608–16

Chen H Z *et al* 2014a AVAZ inversion for fracture weaknesses parameters based on rock physics model *J. Geophys. Eng.* **11** 065007

Chen H Z *et al* 2014b Fracture filling fluids identification using azimuthally elastic impedance based on rock physics *J. Appl. Geophys.* **110** 98–105

Connolly P 1999 Elastic impedance *The Leading Edge* **18** 438–52

Far M E *et al* 2013 Seismic characterization of naturally fractured reservoirs using amplitude versus offset and azimuth analysis *Geophys. Prospect.* **61** 427–47

Hsu C J and Schoenberg M 1993 Elastic waves through a simulated fractured medium *Geophysics* **58** 964–77

Hudson J A 1980 Overall properties of a cracked solid *Math. Proc. Camb. Phil. Soc.* **88** 371–84

Hudson J A 1981 Wave speeds and attenuation of elastic waves in material containing cracks *Geophysics* **64** 133–50

Hudson J A, Liu E and Crampin S 1996 The mechanical properties of materials with interconnected cracks and pores *Geophys. J. Int.* **124** 105–12

Liu E and Martinez A 2012 *Seismic Fracture Characterization* (Houten: European Association of Geoscientists and Engineers)

Martins J L 2006 Elastic impedance in weakly anisotropic media *Geophysics* **71** 2092–6

Mavko G, Mukerji T and Dvorkin J 2009 *The Rock Physics Handbook* (Cambridge: Cambridge University Press)

Mulder W A, Nicoletis L and Alkhalifah T 2006 The EAGE 3D anisotropic elastic modeling project *68th EAGE Conf. & Exhibition*

Pan X P, Zhang G Z and Sun C L 2015 Nonlinear elastic impedance inversion for effective pore-fluid bulk modulus *SEG Expanded Abstracts* 3446–50

Rüger A 1996 Reflection coefficients and azimuthal AVO analysis in anisotropic media *PhD Thesis* Colorado School of Mines

Schoenberg M 1980 Elastic wave behavior across linear slip interfaces *J. Acoust. Soc. Am.* **68** 1516–21

Schoenberg M 1983 Reflection of elastic waves from periodically stratified media with interfacial slip *Geophys. Prosp.* **31** 265–92

Schoenberg M and Douma J 1988 Elastic wave propagation in media with parallel fractures and aligned cracks *Geophys. Prosp.* **36** 571–90

Schoenberg M and Sayers C M 1995 Seismic anisotropy of fractured rock *Geophysics* **60** 204–11

Shaw R K and Sen M K 2006 Use of AVOA data to estimate fluid indicator in a vertically fractured medium *Geophysics* **71** C15–24

Thomsen L 1986 Weak elastic anisotropy *Geophysics* **51** 1954–66

Thomsen L 1995 Elastic anisotropy due to aligned cracks in porous rock *Geophys. Prosp.* **43** 805–30

Thomsen L 2002 *Understanding Seismic Anisotropy in Exploration and Exploitation* (*Distinguished Instructor Series* no 5) (Tulsa, OK: Society of Exploration Geophysicists/European Association of Geoscientists & Engineers) (https://doi.org/10.1190/1.9781560801986)

Tsvankin L and Grechka V 2011 *Seismology of Azimuthally Anisotropic Media and Seismic Fracture Characterization* (*Geophysical References Series* no 17) (Tulsa, OK: Society of Exploration Geophysicists) (https://doi.org/10.1190/1.9781560802839)

Whitcombe D N 2002 Elastic impedance normalization *Geophysics* **67** 60–2

Xu S Y and Payne M A 2009 Modeling elastic properties in carbonate rocks *The Leading Edge* **28** 66–74

Zhang G Z *et al* 2013 Estimation of S-wave velocity and anisotropic parameters using fractured carbonate rock physics model *Chin. J. Geophys.* **56** 1707–15